Supporting information

Combined inhibition of MEK and Plk1 has synergistic anti-tumor activity in NRAS mutant melanoma

Posch C[1,2,3,†,*], Cholewa BD[4,†], Vujic I[1,3], Sanlorenzo M[1,5], Ma J[1], Kim ST[1], Kleffel S[2], Schatton T[2], Rappersberger K[3], Gutteridge R[4], Ahmad N[4], Ortiz-Urda S[1].

[1] University of California San Francisco, Department of Dermatology, Mt. Zion Cancer Research Center, 2340 Sutter Street N461, 94115 San Francisco – USA

[2] Brigham and Women's Hospital, Harvard Medical School, Department of Dermatology, 77 Avenue Louis Pasteur, 02115 Boston – USA

[3] The Rudolfstiftung Hospital, Academic Teaching Hospital, Medical University Vienna, Department of Dermatology, Juchgasse 25, 1030 Vienna – Austria

[4] University of Wisconsin, Department of Dermatology, 7418 Wisconsin Institutes for Medical Research, 1111 Highland Ave, Madison, WI 53705 – USA

[5] Department of Medical Sciences, Section of Dermatology, University of Turin – Italy

[†] Authors contributed equally.

* To whom correspondence should be addressed.

Supporting Material and Methods

Cell Culture, RNA extraction

Human NRAS mutant melanoma cell lines WM3629, WM3060, WM1366 and WM3670 were obtained from the Coriell Institute; Cell lines CHP212 and SW1271 were purchased from ATCC; Cell lines D04, Sk-Mel-2, MM485, MM415, MaMel27II, MaMel30I, MM466, MM537, MaMel144aI, MM3211, Sk-Mel-5, Sk-Mel-28, AV1, AV2, AV5, C918, Mel202, OMM1.3, OMM1 were made available through Boris Bastian at the University of California San Francisco. The cell lines used in this study are known to harbor the mutations listed in table S1. No further authentication was performed. Cell lines D04, Sk-Mel-2, MM485, M415, MaMel27II, MaMel30I, MM466, MM537, MaMel144aI, WM3211, Sk-Mel-5, Sk-Mel-28, Mel202, OMM1.3, OMM1, CHP212 and SW1271 were maintained in RPMI 1640 media supplemented with 10% (vol/vol) fetal bovine serum (FBS). Cell lines WM3629, WM3670, WM3060, WM1366, WM8 were maintained in MCDB153 media supplemented with 20% (vol/vol) Leibovitz's L-15 media, 2% (vol/vol) FBS, and 1.68 mM CaCl2. Cell lines AV1, AV2, AV5 were grown in IMDM medium supplemented with 10% (vol/vol) FBS. All cell lines were incubated at 37°C under 5% CO_2. Infant foreskin derived primary human melanocytes (PHM) were available in our cell repository and grown in M254 medium with HMGS supplements added as recommended by the manufacturer. Cell lines are recognized to harbor the mutations listed in table S1. For total RNA extraction cells were plated 24h prior to extraction, which was carried out using the Qiagen RNAeasy (Qiagen, 74104) extraction kit following the manufacturer's recommendations including DNAse treatment.

qPCR

Total RNA extracts were reverse transcribed using the Quanta q-script cDNA synthesis kit according to the manufacturer's protocol. PCR primers were synthesized by Integrated DNA Technologies (Coralville, IA). Sequences are listed in Table S3. PCR was conducted in triplicate with 20µL reaction volumes of water, Power SYBR® Green, by Applied Biosystems with Rox as a passive reference, 5ng cDNA, and 0.9-0.15mM each primer depending on optimization of the primer set. Sample cDNA was added to the aliquoted SYBR Master Mix and water which was then aliquoted into a 384-well plate. A Non-Template control (NTC) and No-Reverse Transcriptase control (No-RT) were run in duplicate with 20µl reaction volumes. The primers and water were mixed together and added to the NTC, No-RT control, and the Master Mix, water, and cDNA samples in the 384-well plate. PCR was conducted on the ABI 7900HT (Applied Biosystems) using the following cycle parameters: 1 cycle of 95° for 10 minutes, 40 cycles of 95° for 15 seconds, 60° for 1 minute, and 1 cycle of 95° for 15 seconds, 60° for 15 seconds, 95° for 15 seconds. Analysis was carried out using the SDS software (version 2.3) supplied with the ABI 7900HT to determine the Ct values of each reaction. A dissociation curve was run after amplification to ensure the amplification of a single product. Ct-values were determined for three test and three reference reactions in each sample, averaged, and subtracted to obtain the ΔCt [ΔCt = Ct (test locus) – Ct (control locus)]. PCR efficiencies were measured for all custom assays and were greater than or equal to 90%. The relative fold difference was calculated for each primer/probe combination as $2^{-\Delta Ct}$ x 100.

Custom qPCR Array

RNA was isolated as previously described and integrity was verified using a nano chip assay on the Agilent Bioanalyzer. The transcription levels of a gene subset specific to MEK and Plk1 signaling pathways were assessed by a custom 384-well SYBR qPCR array (Bio-Rad, Cat #10025213) with 29 unique assays using ACTB and GAPDH as endogenous reference genes and all manufacturer recommended controls. Each unique assay was run in duplicate per plate and each cell line was run on two plates for a total of 4 replicates per unique assay. The array was ran on a Roche Lightcycler 480 according to manufacturer's protocol and the resultant data was analyzed using the $2^{\Delta\Delta CT}$ method. The average of delta CT and deltadelta CT values are provided in table S5.

Inhibitors, Viability assays, Caspase 3/7 assay, Combination Index Analysis

All inhibitors used in the study were purchased from Selleck Chemicals and ChemieTek. Viability assays were carried out at least in triplicates (incubation for 72h). The relative number of viable cells was assessed using CellTiter-Glo (Promega; G7570). Total luminescence was measured on the SynergyHT plate reader (BioTek) using Gen5 software (Version 1.11.5). Inhibitors were tested covering ranges from 2 – 64nM for the inhibitor JTP-74057 and 15 – 500nM for the inhibitor BI 6727. The concentration of drugs resulting in 50% growth inhibition (IC50) as well as the combination index (CI) determining synergistic effects of drugs in combination was calculated using CalcuSyn software (Biosoft, version 2.1). Synergy was defined following the recommendations of Chou-Talalay (Chou and Talalay 1984). Caspase 3/7 activity was determined by

Caspase-Glo® 3/7 Assay (Promega, G8090) following the manufacturer's instructions. Additionally, the Caspase-Glo® 3/7 Assay (Promega, G8090) was used to determine caspase 3/7 activity in protein extracts from xenograft tumor samples following the manufacturer's recommendations.

Lentiviral production and transduction

HEK 293T cells were passaged to be 30-40% confluent, then Cells were transfected using the $CaPO_4$ method. Briefly, 10µg shRNA plasmid DNA (nonsense shRNA or p53 targeting shRNA) (Sigma Aldrich, MO), 5µg VSV-G and 6µg Δ8.2 plasmids were mixed with sterile ddH_2O to a final volume of 450µl and mixed with 50µl of 2.5 M $CaCl_2$. The DNA mix was bubbled and 500µl 2X HBS (pH 7.05) added drop wise. The transfection mixture was added to its respective plates and incubated overnight. After 24 hours, transfection media was removed and fresh media added. After an additional 24 hours and 48 hours cell media containing shRNA lentivirus was collected and filtered for use. For target cell transduction, Sk-mel-2 cells were passaged to 40% confluency. The viral media was added to cells with 6µg/ml polybrene. After 24 hours of transduction, viral media was removed and fresh media was added. After an additional 24 hours, the media was removed and fresh media containing 2 µg/mL of puromycin was added for 48 hours. Puromycin selection media was refreshed every 48 hours for 4 days total. Following selection, colonies were chosen for subsequent stable line production. NRAS lentiviral transduction was achieved by first cloning the NRAS cDNA into the Gateway entry vector pENTR/D-topo. pENTR/D-topo-NRAS was subjected to site-directed mutagenesis to generate a variety of known NRAS mutants which were then validated

by Sanger sequencing. NRAS cDNAs in pENTR were cloned into the Gateway cloning-enabled destination vector gFG12. Green Fluorescent Protein (GFP) was co-expressed with the different transgenes and used as a transduction efficiency reporter. After lentiviral transduction, cells were grown for 2 weeks followed by cell sorting. Sorted cells displayed comparable NRAS expression levels measured by qPCR.

Cell Cycle Analysis

$1x10^5$ Sk-mel-2 cells were plated and grown in 6-well plates (TPP, CHE) and treated with JTP-74017, BI 6727 or vehicle control. Following treatment, cells were trypsinized for 5 minutes and transferred into 5 mL Falcon tubes containing cultured media. Samples were centrifuged at 1000 RPM for 2 minutes and the supernatant was aspirated prior to the cells being resuspended in ice-cold 100% ethanol added drop-wise while gently vortexing. Samples were stored at -20°C overnight prior to centrifugation and resuspension in 500 µL propidium iodide (PI) buffer (PBS, 50 µg/mL PI, 0.1 mg/mL RNase A, 0.05% Triton-X). Samples were incubated at 37°C for 40 minutes in dark and stored at 4°C until processed by flow cytometry in the FL-2A channel on the Accuri C6 Flow Cytometer (BD Biosciences, CA). Cell cycle histogram overlays were created with FlowJo software (Tree Star, OR) and analysis performed with ModFit LT software (Verity Software, ME).

Cell Cycle Synchronization

Sk-mel-2 cells were plated and grown in 6-well plates (TPP, CHE) until ~40% confluency. For G1/S synchronization, cells were blocked with 2mM thymidine (Sigma,

MO) in MEM for 18 hours, rinsed with PBS and released into fresh MEM for 9 hours. Next, a second thymidine block was conducted for 17 hours. The cells were released from the second block into treated media containing MEKi (JTP-74017) = 20nM; Plk1i (BI 6727) = 100nM, the combination of both, or DMSO control. Following treatment, cells were collected at individual time points (1-24 hours) by trypsinization and processed for cell cycle analysis or protein collection. For G2/M synchronization, a thymidine-nocodazole block was performed following an analogous protocol with an initial thymidine block for 24 hours followed by a 3 hour release and a second block using 100ng/mL nocodazole (Sigma, MO) in MEM for 12 hours. Similarly, the cells were released into treatment and subsequently processed for cell cycle analysis or protein collection.

Immunoblotting

Cells were plated in 6 well plates 24h prior to inhibitor treatment (MEKi (JTP-74017) = 20nM; Plk1i (BI 6727) = 100nM). Following inhibitor incubation for 6h or 24h as indicated, cells were washed with phosphate buffered saline (PBS) and lysed using radio-immunoprecipitation (RIPA) buffer [150 mM NaCl, 1% (vol/vol) Nonidet P-40, 0.5% (wt/vol) sodium deoxycholate, 0.1% (wt/vol) SDS] in 50 mM Tris·HCl (pH 8.0) supplemented with 1x protease and phosphatase inhibitors (78442; Pierce). Protein concentrations were determined using the BCA Protein Assay kit (23235; Pierce). Total protein in 1×Laemmli buffer with 10% 2-mercaptoethanol was separated by SDS/PAGE, transferred for 1 h to a PVDF membrane (IPVH00010; Millipore) by electro blotting with 20% (vol/vol) methanol, and blocked for 1 h in 5% (wt/vol) dry milk/Tris-buffered saline

(TBS)/0.1% (vol/vol) Tween-20. Membranes were incubated overnight at 4°C with primary antibodies following incubation with horseradish peroxidase-conjugated secondary antiserum for 1 h and developed using enhanced chemo-luminescence [32106 (Pierce) or 64 – 201BP (Millipore)]. β–Actin protein expression served as a loading control. P-ERK (4370), p-AKT (4060), p-S6 (4857), Cyclin D1 (2926), Cyclin B1 (12231), Plk1 (4513), p-p53 (9284), p-Rb (8516), Bcl-2 (2872), BAX (2774), p21 (2947), and BIM (2933) were obtained from Cell Signaling Technology, MDM2 (sc-812) and cyclin E (sc-481) were purchased from Santa Cruz Biotechnology, β-Actin was purchased from Sigma Aldrich.

Image processing, statistical analyses

Relative protein expression levels were evaluated by measuring immunoblot band intensities using the image processing and analysis tool ImageJ (1.48v). Statistical significance was evaluated by using independent, two-tailed student's t-tests. Co-occurrence of NRAS and Plk1 genetic alterations was determined via cBioPortal analysis of both genes in the The Cancer Genome Atlas (TCGA) provisional data set for Skin Cutaneous Melanoma (477 samples) with consideration for mutation, putative copy-number alteration, and mRNA expression Z-score (threshold +/- 2.0) (Cerami et al. 2012; Gao et al. 2013).

Mouse xenografts

A total of 5-8*10^6 cells of each cell line was used for subcutaneous injection in CrTac:NCr-*Foxn1*^{nu} mice. Tumor size was calculated using the equation for a triaxial ellipsoid. Inhibitor treatment was initiated when tumors reached a volume of 80-100mm^3. Inhibitor concentrations for single and combination therapy used *in vivo* were 2mg/kg/day for JTP-74057 and 50mg/kg/week for BI 6727. Compounds were administered by oral gavage fife times a week over a period of three weeks. Tumor size changes, body weight and clinical evaluations were carried out three times per week. All animal studies were approved by IACUC/LARC of the University of California San Francisco (AN086990).

Supporting figures

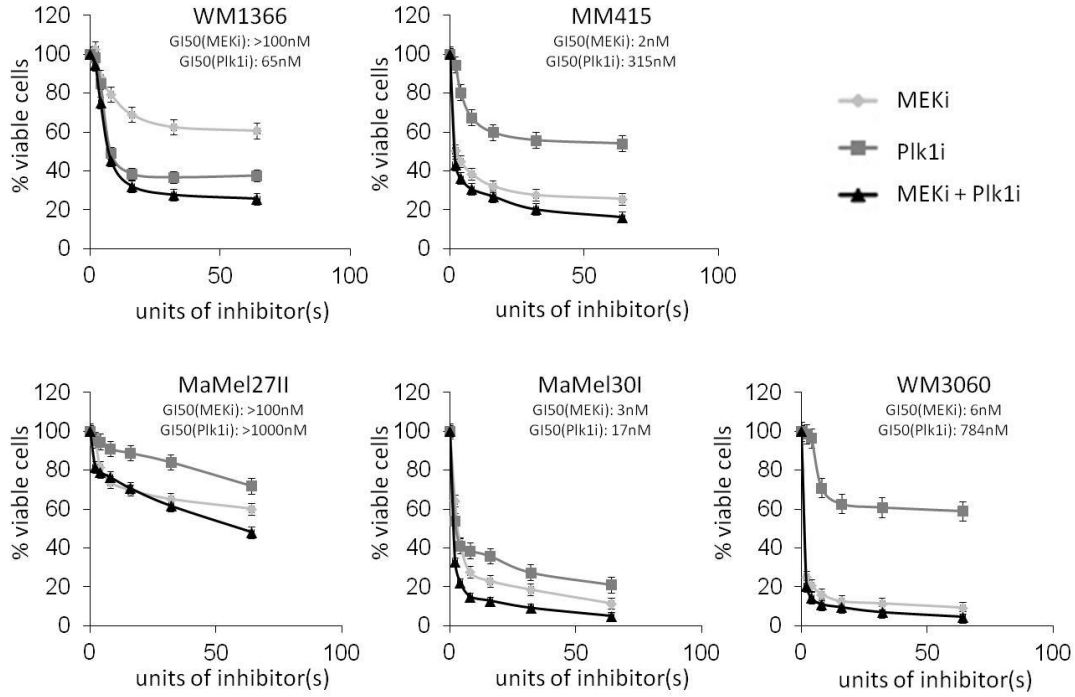

Figure S1. Dose dependent reduction of cell viability with inhibitors of MEK and Plk1. Dose response curves of 5 NRAS mutant melanoma cell lines. WM1366, MM415, MaMel27II, MaMel30I and WM3060 were incubated with inhibitors of MEK, Plk1 or their combination. Graphs showed a greater reduction of cell viability with the MEK/Plk1 combination compared to single inhibitor treatment (N=3, one unit of inhibitor represents 1nM of the MEK inhibitor JTP-74057 and 8nM for the Plk1 inhibitor BI 6727, N=3)

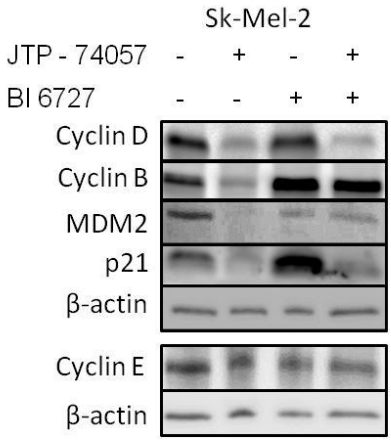

Figure S2. Immunoblot analyses for cell cycle proteins in Sk-Mel-2 cells. Western blot analysis of cell cycle regulators Cyclin D, B and E as well as analysis of p53 target protein p21 and MDM2 following 24h treatment with DMSO control, MEKi (JTP-74057, 20 nM), Plk1i (BI 6727, 100 nM), or Plk1i + MEKi.

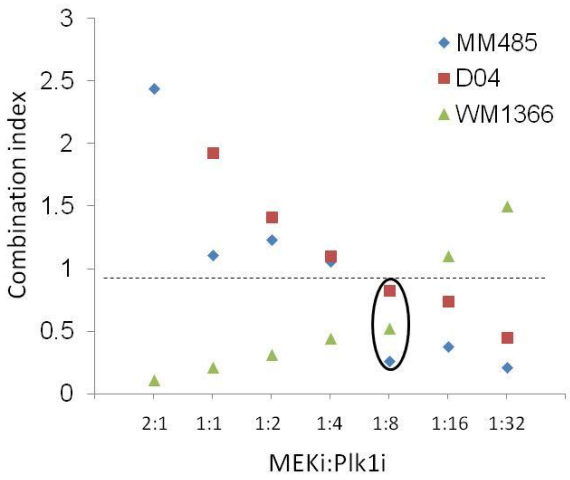

Figure S3. Synergistic inhibition of NRAS mutant cells at a molar ratio of Mek:Plk1=1:8. Combination Index (CI) for NRAS mutant cell lines MM485, D04 and WM1366 at different ratios of MEKi/Plk1i. All human, NRAS mutant melanoma cell lines were synergistically inhibited when a molar ratio of MEKi:Plk1i=1:8 was used (table S2).

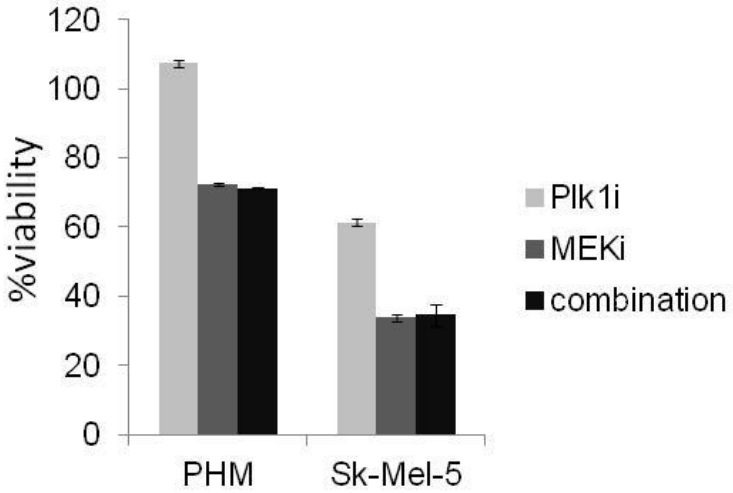

Figure S4. No additional reduction of viability with the MEK/Plk1 combination in PHM and the BRAF(V600E) mutant cell line Sk-Mel-5 compared to MEKi treatment alone. Relative viability of non-transformed human melanocytes and the BRAF(V600E) mutant melanoma cell line Sk-Mel-5 incubated with the MEKi (32nM), the Plk1i (256nM) or the combination of both inhibitors compared to vehicle treated controls. (N=3; error bars=SD)

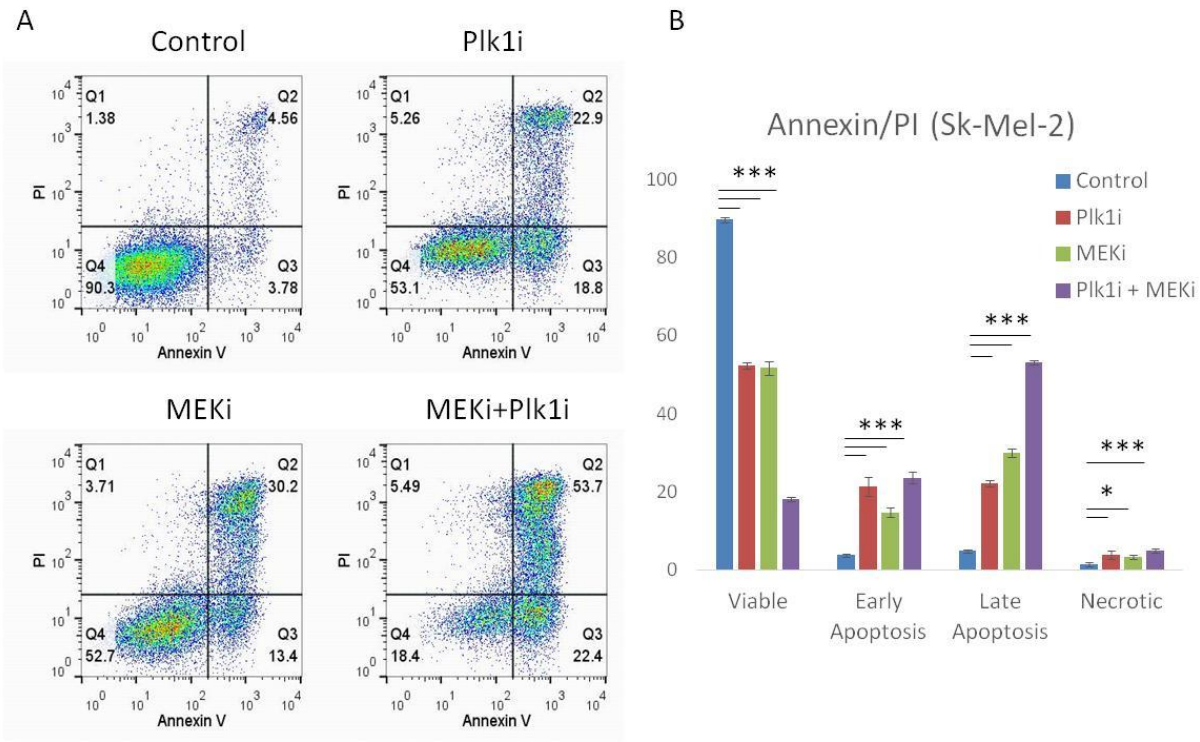

Figure S5A. Induction of apoptosis in Sk-Mel-2 cells with the MEK/Plk1 combination. Representative sample of flow cytometric analysis for Sk-Mel-2 cells stained with Annexin V and propidium iodide as markers for induction of apoptosis and cell death, respectively, following treatment with DMSO control, MEKi (JTP-74057, 20 nM), Plk1i (BI 6727, 100 nM), or Plk1i + MEKi. **S5B.** Mean value of individual flow cytometric analyses (N=3) representing viable (Q4), early apoptotic (Q3), late apoptotic (Q2), and necrotic (Q1) populations (***$p<0.001$, *$p<0.05$).

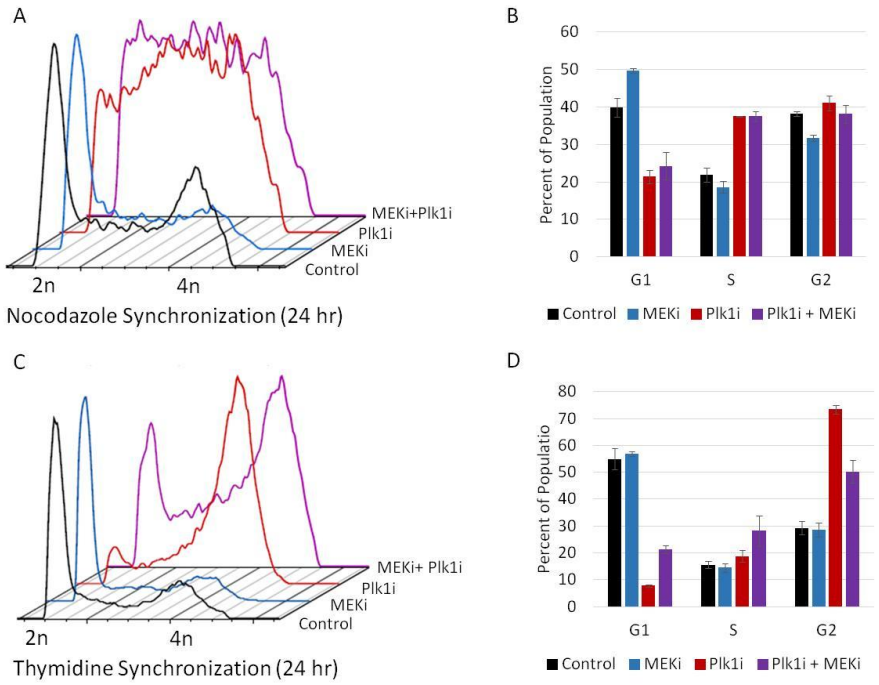

Figure S6A. Cell cycle analyses of Sk-Mel-2 cells 24 hours after synchronization. Overlaid histogram analysis of DNA content as determined by propidium iodide in Sk-mel-2 cells treated with DMSO control, MEKi (JTP-74057, 20 nM), Plk1i(BI 6727, 100 nM), or Plk1i + MEKi for 24 hours following G2/M synchronization via thymidine-nocodazole block. **S5B.** Mean value of individual flow cytometric analyses of the cell cycle following nocodazole synchronization. **S5C.** Overlaid histograms for Plk1i and MEKi treatments following late G1 synchronization via double thymidine block. **S6D.** Mean value of individual flow cytometric analyses of the cell cycle following thymidine synchronization.

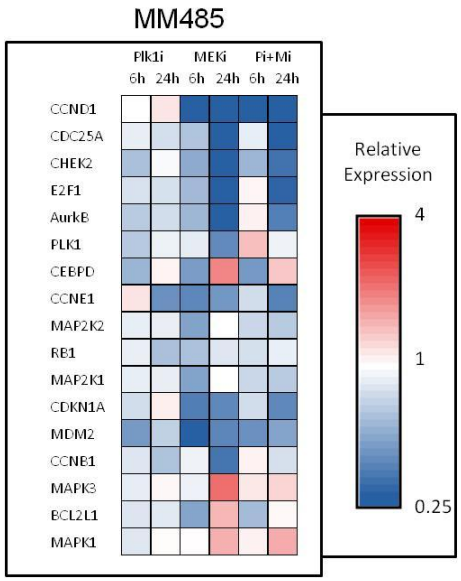

Figure S7. Regulation of cell cycle genes, and p53/p21 signaling members with inhibitors of MEK and Plk1. Reduction of MDM2, RB1, CCNE1 and induction of CCND1 and CDKN1A by Plk1 after 24h of inhibitor treatment. Reduction of CCND1, CDC25A, CHEK2, E2F1, AurkB, and CCNB1 as well as induction of CEBPD, MAPK3, BCL2L1, and MAPK1 after 24h of MEK inhibitor treatment. Dual inhibition with MEK/Plk1 showed less induction of CEBPD and MAPK3 compared to MEKi treatment alone. Additionally, MAP2K2 and MAP2K1 were reduced by the MEK/Plk1 combination compared to MEKi treatment alone after 24h of inhibitor treatment.

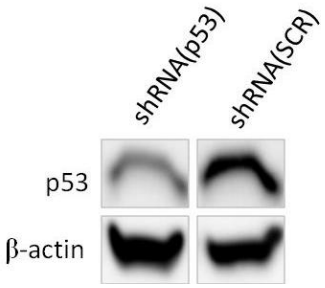

Figure S8. Stable knockdown of p53 in Sk-Mel-2 cells. Protein levels of p53 and β-actin in Sk-Mel-2 cells. All samples were analyzed on one and the same blot, β-actin served as a loading control.

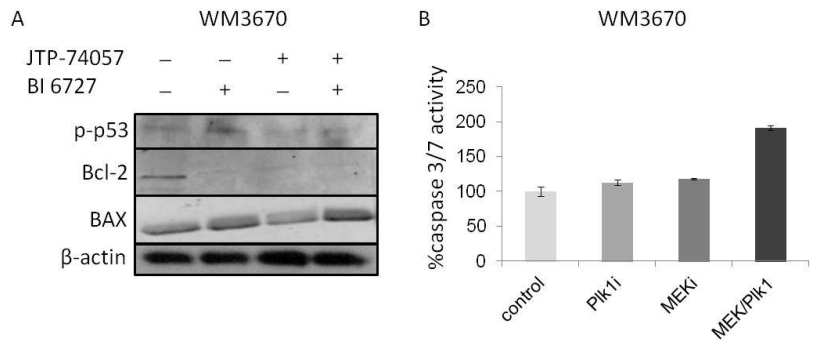

Figure S9A. Induction of apoptosis in WM3670 mouse tumors with the MEK/Plk1 combination. Immunoblot analyses of WM3670 mouse tumors indicating the induction of p-p53 with Plk1 inhibition, the induction of the pro-apoptotic marker BAX and the reduction of the anti-apoptotic marker Bcl-2 with the MEK/Plk1 combination. **S9B.** Caspase 3/7 activity in protein extracts from mouse xenografts treated with the indicated conditions.

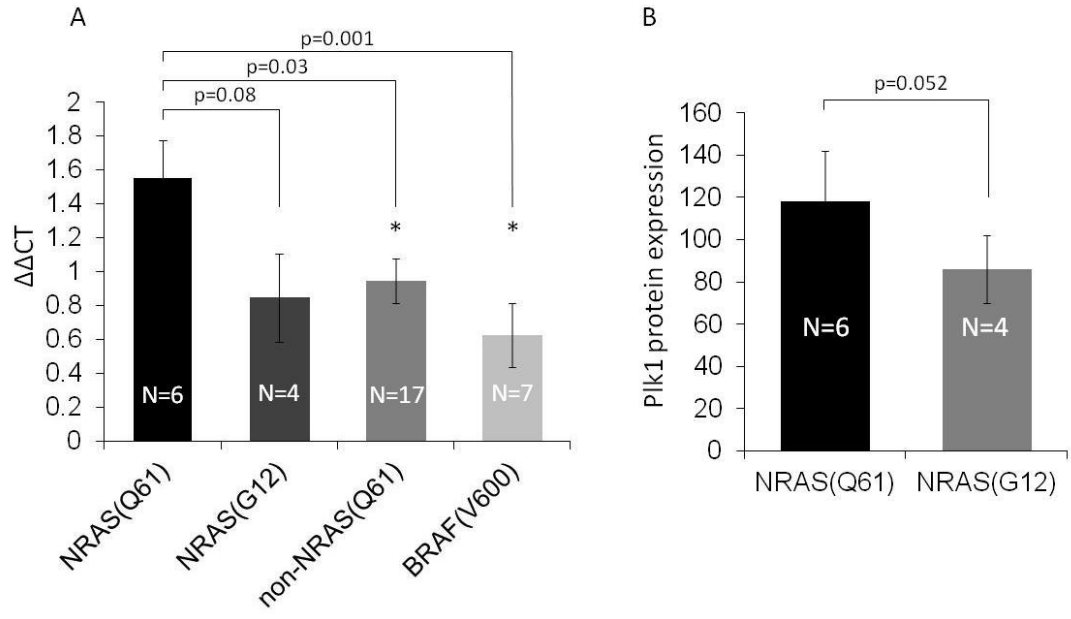

Figure S10A. High Plk1 mRNA and protein levels in NRAS(Q61) mutant cells. Plk1 mRNA expression in a collection of 23 human melanoma cell lines. **S10B.** Relative protein expression measured by the intensity of immunoblot bands compared to β-actin between 6 NRAS(Q61) and 4 NRAS(G12) mutant cell lines. (error bars=SD; * indicates $p<0.05$)

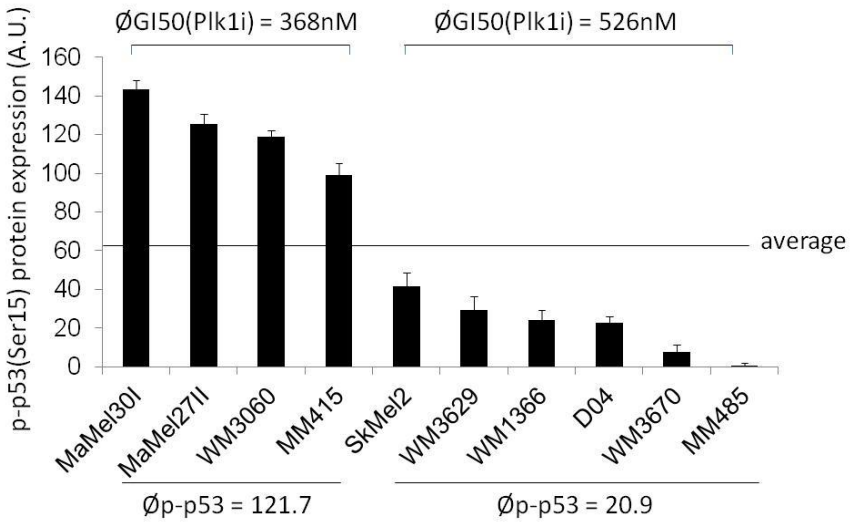

Figure S11. NRAS mutant melanoma cells expressing high levels of p-p53 require less Plk1 inhibitor for equipotent growth inhibition. Relative p-p53(Ser15) protein expression to β-actin controls in 10 NRAS mutant melanoma cell lines. There was a trend that cells with low p-p53(Ser15) protein expression require higher Plk1i concentrations to reach GI50 compared to cells with high p-p53(Ser15) expression. (Bars represent the average p-p53(Ser15) protein expression of the respective cell line (A.U.); error bars=SD; N=3)

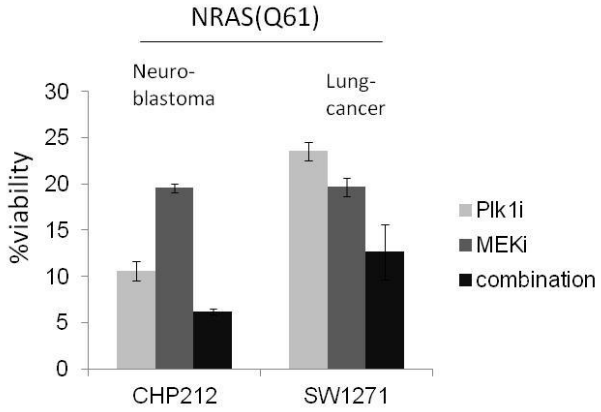

Figure S12. The MEK/Plk1 combination effectively reduces cell viability in NRAS mutant neuroblastoma and lung cancers cells. Relative viability of one NRAS mutant neuroblastoma (CHP212) and one NRAS mutant lung cancer (SW1271) cell line in response to Plk1i, MEKi or to the MEK/Plk1 inhibitor combination. (MEKi(JTP-74057)=32nM; Plk1i(BI 6727)=256nM; error bars=SD; N=3)

Table S1. Mutation status and relative expression of Plk1 of cell lines used in this study. (WT: wild type for BRAF, NRAS, C-KIT, GNAQ/GNA11, Plk1 hotspot mutations)

Cell line	mutation	Plk1 (exon5,9)	CDKN2A	ΔΔCT Plk1
D04	NRAS(Q61L)	WT	homozyg. deletion	1.312
MM415	NRAS(Q61L)	WT	wild type	1.817
MM485	NRAS(Q61R)	WT	mutant (W110Stop)	2.310
WM1366	NRAS(Q61L)	WT	partial deletion	0.830
Sk-Mel-2	NRAS(Q61K)	WT	wild type	1.121
WM3060	NRAS(Q61K)	WT	mutant	1.912
MaMel27II	NRAS(G12D)	WT	wild type	1.417
MaMel30I	NRAS(G13D) BRAF(D594N)	WT	homozyg. Deletion	0.179
WM3629	NRAS(G12D) BRAF(D549G)	Plk1(C633T)	wild type	1.027
WM3670	NRAS(G12D) BRAF(G469E)	WT	wild type	0.762
Ma-Mel-144aI	C-KIT(S476I)	WT	-	1.600
WM3211	C-KIT(L576P)	-	-	1.777
Sk-Mel-5	BRAF(V600E)	WT	-	0.660
Sk-Mel-28	BRAF(V600E)	-	-	0.860
AV1	BRAF(V600E)	-	-	0.039
AV2	BRAF(V600E)	-	-	0.152
AV5	BRAF(K601E)	-	-	1.561
MM466	BRAF(V600E)	-	-	0.605
MM537	BRAF(V600E)	-	-	0.491
C918	WT	-	-	0.871
Mel202	GNAQ(Q209L)	-	-	1.226
OMM1.3	GNAQ(Q209P)	WT	-	1.452
OMM1	GNA11(Q209L)	WT	-	1.416
PHM(E)	WT	-	-	0.304
PHM(G12)	NRAS(G12V)	-	-	0.187
PHM(N24)	NRAS(N24I)	-	-	0.274
PHM(Q61)	NRAS(Q61L)	-	-	0.504
CHP212	NRAS(Q61K)	WT	-	-
SW1271	NRAS(Q61R)	WT	-	-

Table S2. Concentration for 50% of maximal inhibition of cell proliferation (GI50), dose reduction index (DRI) and combination index (CI) for 10 NRAS mutant melanoma cell lines at a ratio of MEKi:PLK1i = 1:8. (N=3)

Cell line	MEKi JTP-74057	Plk1i BI 6727	DRI(MEKi) JTP-74057	DRI(Plk1i) BI 6727	CI value at FA50	p-value
D04	1nM	29nM	1.63	4.64	0.83	0.001
MM415	2nM	315nM	2.04	39.82	0.52	0.003
MM485	4nM	>1000nM	3.94	166.97	0.26	0.013
WM1366	>100nM	65nM	61.35	1.92	0.54	0.045
Sk-Mel-2	19nM	58nM	10.03	3.91	0.38	0.023
WM3060	6nM	784nM	20.81	153.19	0.01	0.001
MaMel27II	>100nM	>1000nM	2.75	5.29	0.55	0.011
MaMel30I	3nM	17nM	5.60	3.91	0.43	0.012
WM3629	7nM	292nM	2.51	13.02	0.48	0.004
WM3670	78nM	>1000nM	3.13	7.40	0.45	0.008

Table S3. Interpretation of CI values following the recommendations of Chou-Talalay (Chou and Talalay 1984).

Range of CI	Symbol	Description
<0.1	+++++	Very strong synergism
0.1-0.3	++++	Strong synergism
0.3-0.7	+++	Synergism
0.7-0.85	++	Moderate synergism
0.85-0.9	+	Slight synergism
0.9-1.1	+/-	Nearly additive
1.1-1.2	-	Slight antagonism
1.2-1.45	--	Moderate antagonism
1.45-3.3	---	Antagonism
3.3-10	----	Strong antagonism
>10	-----	Very strong antagonism

Table S4. qPCR primer sequences for Plk1 and β-actin detailed from 5' to 3'.

target	forward	reverse
PLK1	CCCCTCACAGTCCTCAATAA	AATAGTCCACCCACTTGCTG
β-actin	TACGCCAACACAGTGCTGTCT	GCCGATCCACACGGAGTACT

Table S5. Delta CT and deltadelta CT values of the custom mRNA array at the indicated time points for the respective cell lines. Values represent the average of 4 replicates.

MM485 – 6h incubation

Δct	Control	MEKi	Plki	MEKi + Plki	$2^{-\Delta\Delta ct}$	MEKi	Plki	MEKi + Plki
AurkB	6.378	6.975	6.781	6.152	AurkB	0.661	0.757	1.170
CCNB1	4.548	4.630	4.721	4.335	CCNB1	0.945	0.887	1.160
CCND1	3.963	6.640	3.956	6.221	CCND1	0.156	1.005	0.209
CCNE1	8.477	9.655	8.078	8.722	CCNE1	0.442	1.318	0.844
CDKN1A	8.823	10.170	9.072	9.071	CDKN1A	0.393	0.842	0.843
E2F1	7.493	8.059	7.705	7.344	E2F1	0.676	0.864	1.109
MAP2K1	5.617	6.119	5.618	5.834	MAP2K1	0.706	0.999	0.860
MAP2K2	4.070	4.888	4.188	4.370	MAP2K2	0.567	0.921	0.812
MAPK1	4.926	4.889	5.092	4.700	MAPK1	1.026	0.891	1.170
MAPK3	6.223	6.309	6.348	5.877	MAPK3	0.943	0.917	1.271
MDM2	6.706	8.882	7.628	7.755	MDM2	0.221	0.528	0.483
PLK1	7.626	7.758	8.046	6.807	PLK1	0.913	0.747	1.764
RB1	5.477	5.963	5.588	5.701	RB1	0.714	0.926	0.856
CEBPD	7.970	8.865	8.583	8.907	CEBPD	0.538	0.654	0.522
CDC25A	7.381	7.850	7.495	7.501	CDC25A	0.722	0.924	0.920
CHEK2	9.967	10.688	10.471	10.567	CHEK2	0.607	0.705	0.660
BCL2L1	6.923	7.718	7.111	7.470	BCL2L1	0.577	0.878	0.685

MM485 – 24h incubation

Δct	Control	MEKi	Plki	MEKi + Plki	$2^{-\Delta\Delta ct}$	MEKi	Plki	MEKi + Plki
AurkB	6.128	8.987	6.376	7.444	AurkB	0.138	0.843	0.402
CCNB1	4.424	5.911	4.903	4.647	CCNB1	0.357	0.718	0.857
CCND1	4.444	8.696	4.052	8.804	CCND1	0.052	1.312	0.049

CCNE1	8.048	9.000	9.099	9.305	CCNE1	0.517	0.483	0.418
CDKN1A	10.151	11.317	9.889	11.328	CDKN1A	0.446	1.199	0.442
E2F1	8.148	10.947	8.366	10.008	E2F1	0.144	0.860	0.275
MAP2K1	5.648	6.020	5.472	6.229	MAP2K1	0.772	1.129	0.668
MAP2K2	4.054	4.051	4.169	4.452	MAP2K2	1.002	0.924	0.759
MAPK1	5.003	4.053	4.952	4.019	MAPK1	1.932	1.036	1.978
MAPK3	6.278	4.841	6.136	5.682	MAPK3	2.708	1.104	1.512
MDM2	7.588	8.787	7.941	8.395	MDM2	0.436	0.783	0.572
PLK1	8.436	9.573	8.526	8.514	PLK1	0.455	0.940	0.947
RB1	5.501	5.677	6.006	5.612	RB1	0.885	0.705	0.926
CEBPD	8.181	6.900	8.002	7.442	CEBPD	2.430	1.132	1.669
CDC25A	7.396	10.657	7.626	9.482	CDC25A	0.104	0.853	0.236
CHEK2	10.141	12.491	10.172	11.679	CHEK2	0.196	0.978	0.344
BCL2L1	6.948	6.057	7.106	6.824	BCL2L1	1.854	0.896	1.089

D04 – 6h incubation

Δct	Control	MEKi	Plki	MEKi + Plki	$2^{-\Delta\Delta ct}$	MEKi	Plki	MEKi + Plki
AurkB	6.987	7.131	7.405	6.708	AurkB	0.905	0.749	1.214
CCNB1	3.805	3.694	3.532	4.020	CCNB1	1.080	1.208	0.862
CCND1	5.857	7.646	6.102	7.213	CCND1	0.289	0.844	0.391
CCNE1	7.500	7.356	6.927	7.498	CCNE1	1.105	1.487	1.001
CDKN1A	8.912	8.469	8.917	7.768	CDKN1A	1.360	0.996	2.211
E2F1	7.632	7.391	7.605	7.723	E2F1	1.182	1.019	0.939
MAP2K1	5.982	6.036	6.012	5.945	MAP2K1	0.963	0.979	1.026
MAP2K2	5.150	5.091	5.222	4.725	MAP2K2	1.041	0.951	1.342
MAPK1	4.525	4.229	4.480	4.285	MAPK1	1.228	1.032	1.181
MAPK3	7.412	7.009	6.889	6.678	MAPK3	1.323	1.437	1.664

MDM2	6.695	7.156	7.142	6.755	MDM2	0.726	0.733	0.959
PLK1	9.800	10.226	10.195	8.873	PLK1	0.744	0.760	1.901
RB1	6.760	6.759	6.687	6.950	RB1	1.001	1.051	0.876
CEBPD	5.275	5.684	5.672	6.098	CEBPD	0.753	0.759	0.565
CDC25A	7.500	8.151	7.845	8.118	CDC25A	0.637	0.787	0.652
CHEK2	10.780	9.919	10.495	9.918	CHEK2	1.816	1.218	1.818
BCL2L1	5.877	6.151	5.982	6.471	BCL2L1	0.827	0.930	0.663

D04 – 24h incubation

Δct	Control	MEKi	Plki	MEKi + Plki	$2^{-\Delta\Delta ct}$	MEKi	Plki	MEKi + Plki
AurkB	6.104	7.617	7.024	7.157	AurkB	0.350	0.528	0.482
CCNB1	3.904	4.931	3.807	3.707	CCNB1	0.491	1.069	1.146
CCND1	6.061	6.104	5.420	6.278	CCND1	0.971	1.560	0.860
CCNE1	6.816	7.486	7.297	7.385	CCNE1	0.629	0.717	0.674
CDKN1A	7.716	6.697	6.635	6.355	CDKN1A	2.027	2.117	2.570
E2F1	6.709	8.536	7.682	7.987	E2F1	0.282	0.509	0.412
MAP2K1	5.714	5.941	5.677	5.782	MAP2K1	0.854	1.026	0.954
MAP2K2	4.729	5.066	4.877	4.827	MAP2K2	0.792	0.902	0.934
MAPK1	4.266	3.511	4.515	3.757	MAPK1	1.688	0.842	1.423
MAPK3	6.356	5.084	6.477	5.827	MAPK3	2.416	0.920	1.443
MDM2	6.629	6.204	6.077	5.852	MDM2	1.342	1.466	1.713
PLK1	9.666	11.156	9.917	10.135	PLK1	0.356	0.841	0.723
RB1	6.354	6.196	6.945	6.485	RB1	1.116	0.664	0.913
CEBPD	5.174	3.471	5.217	4.640	CEBPD	3.255	0.971	1.448
CDC25A	7.036	9.019	8.050	8.982	CDC25A	0.253	0.495	0.260
CHEK2	8.919	10.000	9.855	10.155	CHEK2	0.473	0.523	0.425
BCL2L1	6.234	5.229	6.047	5.727	BCL2L1	2.007	1.138	1.421

Sk-Mel-2 – 6h incubation

Δct	Control	MEKi	Plki	MEKi + Plki	$2^{-\Delta\Delta ct}$	MEKi	Plki	MEKi + Plki
AurkB	6.656	7.050	6.513	6.162	AurkB	0.761	1.104	1.409
CCNB1	4.436	3.878	3.785	3.742	CCNB1	1.472	1.570	1.618
CCND1	4.378	5.855	3.614	5.672	CCND1	0.359	1.698	0.408
CCNE1	9.049	9.438	8.230	8.512	CCNE1	0.763	1.763	1.451
CDKN1A	6.429	10.276	6.518	5.557	CDKN1A	0.069	0.940	1.830
E2F1	7.739	7.660	7.148	7.374	E2F1	1.056	1.506	1.287
MAP2K1	5.309	5.575	5.315	5.492	MAP2K1	0.832	0.995	0.881
MAP2K2	4.586	4.975	4.498	4.457	MAP2K2	0.764	1.063	1.094
MAPK1	3.714	3.128	3.663	3.034	MAPK1	1.500	1.036	1.601
MAPK3	7.456	6.875	6.955	6.592	MAPK3	1.496	1.415	1.821
MDM2	5.091	7.849	5.518	5.849	MDM2	0.148	0.744	0.591
PLK1	10.301	11.519	10.220	9.349	PLK1	0.430	1.058	1.934
RB1	6.979	7.423	7.153	6.922	RB1	0.735	0.886	1.040
CEBPD	6.081	6.680	6.065	6.582	CEBPD	0.660	1.011	0.707
CDC25A	8.185	10.870	10.160	9.334	CDC25A	0.156	0.254	0.451
CHEK2	9.949	17.376	8.509	9.129	CHEK2	0.006	2.713	1.765
BCL2L1	5.909	5.588	6.113	5.917	BCL2L1	1.248	0.868	0.994

Sk-Mel-2 – 24h incubation

Δct	Control	MEKi	Plki	MEKi + Plki	$2^{-\Delta\Delta ct}$	MEKi	Plki	MEKi + Plki
AurkB	6.258	8.890	6.065	7.568	AurkB	0.161	1.143	0.403
CCNB1	5.198	6.779	4.085	4.458	CCNB1	0.334	2.163	1.670
CCND1	3.758	7.956	3.867	6.853	CCND1	0.054	0.927	0.117
CCNE1	8.460	8.061	9.337	8.381	CCNE1	1.318	0.545	1.057
CDKN1A	5.323	4.150	5.125	4.686	CDKN1A	2.254	1.147	1.555

E2F1	6.880	10.259	7.850	8.658	E2F1	0.096	0.511	0.292
MAP2K1	5.648	5.686	5.877	5.303	MAP2K1	0.974	0.853	1.270
MAP2K2	4.500	4.344	4.730	4.418	MAP2K2	1.114	0.853	1.059
MAPK1	3.950	1.751	3.755	2.231	MAPK1	4.591	1.145	3.293
MAPK3	6.615	5.184	6.210	5.651	MAPK3	2.697	1.325	1.952
MDM2	4.880	3.950	4.680	4.201	MDM2	1.905	1.149	1.602
PLK1	7.093	9.455	6.374	7.643	PLK1	0.194	1.646	0.683
RB1	6.733	6.741	7.102	6.586	RB1	0.994	0.774	1.107
CEBPD	5.748	5.686	6.052	5.738	CEBPD	1.043	0.810	1.007
CDC25A	8.568	12.789	9.170	10.473	CDC25A	0.054	0.659	0.267
CHEK2	7.898	10.060	7.849	9.728	CHEK2	0.223	1.035	0.281
BCL2L1	6.328	4.654	6.017	5.133	BCL2L1	3.191	1.240	2.289

References

Cerami, E, Gao, J, Dogrusoz, U, *et al.* (2012). The cBio cancer genomics portal: an open platform for exploring multidimensional cancer genomics data. *Cancer Discov* 2: 401–4.

Chou, TC, Talalay, P (1984). Quantitative analysis of dose-effect relationships: the combined effects of multiple drugs or enzyme inhibitors. *Adv Enzyme Regul* 22: 27–55.

Gao, J, Aksoy, BA, Dogrusoz, U, *et al.* (2013). Integrative analysis of complex cancer genomics and clinical profiles using the cBioPortal. *Sci Signal* 6: pl1.